

The eV-Scale Sterile Neutrino and Neutrinoless Double Beta Decay

Priya*, Simran Arora† and B. C. Chauhan‡

Department of Physics and Astronomical Science, Central University of Himachal Pradesh, Dharamshala (HP) 176215, India

Abstract

In short-baseline experiments such as LSND and MiniBooNE, an excess of electron neutrinos has been observed, originating from a muon neutrino beam. To address this anomaly, in the line of many works, we investigate various neutrino mixing schemes involving eV-scale sterile neutrinos alongside three active neutrinos. Using updated experimental and global fit data, we studied neutrinoless double beta decay for three different schemes such as 3+1, 1 + 3, and 2 + 2, which involve one sterile neutrino and three active neutrinos. We have done analysis of these schemes for normal hierarchy (NH) as well as for inverted hierarchy (IH) frameworks, and constrained the sterile neutrino mass in light of current and future neutrinoless double beta decay experiments. The 3+1 scheme is found to be the most viable and at the level of 3σ the mass of sterile neutrino with respect to the lightest neutrino mass (m_{lightest}) is restricted to 4.75 eV for the NH and 4.72 eV for the IH. Additionally, the limits on the sum of four neutrino masses are determined to be 4.81 eV for the normal hierarchy and 4.78 eV for the inverted hierarchy. The updated analysis of all these schemes would help us in understanding physics governing neutrinoless double beta decay and limit on the mass of sterile neutrinos.

Keywords: eV scale sterile neutrinos, neutrinoless double beta decay.

1 Introduction

The purpose of neutrinoless double beta decay ($0\nu\beta\beta$) studies is far more basic than just measuring neutrino mass; it is the search for lepton number violation and for Majorana nature of the neutrinos [1,2]. A special case of double beta decay known as ‘neutrinoless double beta decay’ occurs when no neutrinos (or antineutrinos) are produced as products [3]. The reaction governing $0\nu\beta\beta$ is given by

$$(A, Z) \rightarrow (A, Z + 2) + 2e^-,$$

where the lepton number is violated by 2 units ($\Delta L = 2$) [4]. A number of experiments are now underway or are scheduled to begin soon in the search of neutrinoless double beta decay [5–14]. The

*kashyappriya963@gmail.com

†009simranarora@gmail.com

‡chauhan@associates.iucaa.in

KamLAND-Zen experiment currently holds the best position in establishing the experimental limit for $0\nu\beta\beta$, which search the decay in ^{136}Xe -doped liquid scintillator. It has established a lower limit for the $0\nu\beta\beta$ decay half life of $\tau \geq 3.8 \times 10^{26}$ years at a 90% confidence level (CL). This provides upper limit of effective Majorana mass parameter ($m_{\beta\beta}$) in the range 28–122 meV at 90% CL [7,14].

In the Standard Model of particle physics, there are three known types of neutrinos: the electron neutrino, muon neutrino, and tau neutrino. These are called ‘active’ neutrinos because they interact with other particles through the weak force and oscillate due to the mass squared differences, for example, of the order 10^{-5}eV^2 and 10^{-3}eV^2 [15]. Many different scientific evidences have been pointing towards the possible existence of something called ‘sterile neutrinos’ at a specific energy scale [16]. These hints come from various experiments and observations, including the Liquid Scintillator Neutrino Detector (LSND) [17, 18], Gallium experiments [19, 20], T2K experiment [21], and the MiniBooNE experiment [22–24]. The LSND experiment was a short-baseline experiment with the baseline length $\sim 30\text{m}$, that investigates $\bar{\nu}_\mu \rightarrow \bar{\nu}_e$ oscillations and reported an excess of $\bar{\nu}_e$ -like events [25]. It observed an event excess with a significance of 3.8σ . Although, a similar experiment, KARMEN, with the baseline length $\sim 17\text{m}$ also studied the oscillation channel $\bar{\nu}_\mu \rightarrow \bar{\nu}_e$, but did not confirm the LSND anomaly [26, 27].

The MiniBooNE experiment, designed to confirm the LSND anomaly, also reports a low-energy excess in the electron like events. The MicroBooNE experiment was established to test this excess using a liquid argon time projection chamber [28]. The first three years of MicroBooNE data show no evidence of sterile neutrino oscillations and are consistent with the 3ν hypothesis at the 1σ level [29, 30]. However, see Ref. [31], when focused on the disappearance of electron neutrinos across four channels in MicroBooNE data, a hint of oscillations was observed. A strong signal (2.4σ) was observed in the Wire-Cell analysis, with preferred parameters $\sin^2(2\theta_{14}) = 0.35_{-0.16}^{+0.19}$ and $\Delta m_{41}^2 = 1.25_{-0.39}^{+0.74} \text{eV}^2$.

The Baksan Experiment on Sterile Transitions (BEST) investigated the gallium anomaly and reported best fit parameters $\Delta m^2 = 3.3_{-2.3}^{+\infty} \text{eV}^2$ and $\sin^2 2\theta = 0.42_{-0.17}^{+0.15}$, consistent with SAGE and GALLEX with higher significance [32]. Similarly, GALLEX/GNO and SAGE observed this anomaly at a 3.2σ confidence level [33]. However, the NEUTRINO-4 experiment reported evidence for active-sterile oscillations at the 2.9σ level with best-fit parameters $\Delta m_{14}^2 = (7.3 \pm 1.17) \text{eV}^2$ and $\sin^2 2\theta = 0.36 \pm 0.12$ [34]. On the other hand, several high-precision reactor antineutrino experiments contradict these claims [35]. The DANSS experiment found no statistically significant evidence for sterile neutrinos, with the best-fit point in the 4ν case having only 1.3σ significance [36]. The NEOS experiment also reported no strong evidence for $3+1$ neutrino oscillations, constraining the mixing parameter to $\sin^2 2\theta_{14} < 0.1$ for Δm_{41}^2 in the range $0.2\text{--}2.3 \text{eV}^2$ at a 90% confidence level [37]. Similarly, the Double Chooz experiment found no indication of sterile neutrino mixing and set exclusion limits in the mass range $5 \times 10^{-3} \text{eV}^2 \lesssim \Delta m_{41}^2 \lesssim 3 \times 10^{-1} \text{eV}^2$, for mixing angle $\sin^2 2\theta_{14} \gtrsim 0.02$, further constraining the allowed parameter space for light sterile neutrinos [38]. The RENO experiment provides the most stringent limits on sterile neutrino mixing in the region $\Delta m_{41}^2 \lesssim 0.002 \text{eV}^2$, based on precise measurements of electron antineutrino ($\bar{\nu}_e$) disappearance [39]. The Daya Bay experiment has excluded light sterile neutrino mixing with $\sin^2 2\theta_{14} \gtrsim 0.01$ at the 95% confidence level in the mass range $0.01 \text{eV}^2 \lesssim \Delta m_{41}^2 \lesssim 0.1 \text{eV}^2$ [40].

The investigation of sterile neutrinos may shed light on why ordinary neutrinos have mass. Three scales of neutrino mass squared differences $\Delta m_{\text{solar}}^2$, Δm_{atm}^2 [41] and Δm_{LSND}^2 [42] have been found through solar, atmospheric neutrino oscillation experiments and LSND collaboration. These three

mass-squared differences are required to explain the active-sterile neutrino framework. This type of work has been widely explored in the literature [43–58].

In our work, motivated by the updated global data of short baseline neutrino experiments, reactor experiments, and updates of the experiments on the nature and mass scale of neutrinos, we have investigated the third mass squared difference in the 3σ range, i.e., $1.1 - 2.4 eV^2$ and at the best-fit value, i.e., $1.73 eV^2$ [45]. We also constrained the mass of light sterile neutrinos and the sum of four neutrino masses in light of data from the current and future generations of experiments.

The most general case involving sterile neutrinos is discussed in the literature, where three active neutrinos are considered as light mass eigenstates and the sterile neutrino is regarded as a heavier mass eigenstate. The lightest neutrino mass, effective Majorana mass, mass of sterile neutrino and sum of neutrino masses have also been constrained in various works. Readers can refer to [47–49] for detailed study.

In this work, we have considered different active-sterile schemes for analysis of effective Majorana mass in $0\nu\beta\beta$ in light of current and future experiments. We have taken three possible schemes with three active neutrinos and one sterile neutrino. We have identified the most viable scheme by exploring the third mass squared difference and obtained constraints on the mass of sterile neutrinos. Based on our current understanding of neutrino mass squared differences and mixing angles it is possible to analyse the range of values for the effective Majorana mass $m_{\beta\beta}$ in neutrinoless double-beta decay as a function of the absolute scale of neutrino masses [42].

The paper is organised as follow: In Section 2, we discuss about three different active-sterile neutrino schemes and checked the viability in light of existing bounds. In Section 3, we discuss the effective Majorana mass in 3+1 scheme for normal and inverted hierarchies. The details of the numerical analysis and interpretation of the phenomenological results are discussed in Section 4. Finally, in Section 5 the conclusions are elucidated.

2 Different Possible Active-Sterile Neutrino Schemes

In this section, we describe different neutrino mixing schemes possible through the various combination of four neutrinos i.e. three active neutrinos and one sterile neutrino: 3+1, 1+3, and 2+2 [50]. In the 3+1 scheme, three active neutrinos behave as light mass eigenstates, while the sterile neutrino acts as a heavy mass state. We have explored possible mass squared differences between the active neutrinos in sub schemes 1 and 2. For the 1+3 scheme, one light mass eigenstate is accompanied by three heavy mass eigenstates. Sub schemes 3 and 4 consider the sterile neutrino as a heavy mass eigenstate along with two active neutrinos, while sub schemes 5 and 6 involve the sterile neutrino as an extra light mass eigenstate, with the three active neutrinos being heavier than this light mass eigenstate shown in Fig. 1. In 2+2 scheme, two active neutrino behave as light mass and one active and one sterile neutrino behave as heavy mass eigenstates (sub schemes 7 and 8).

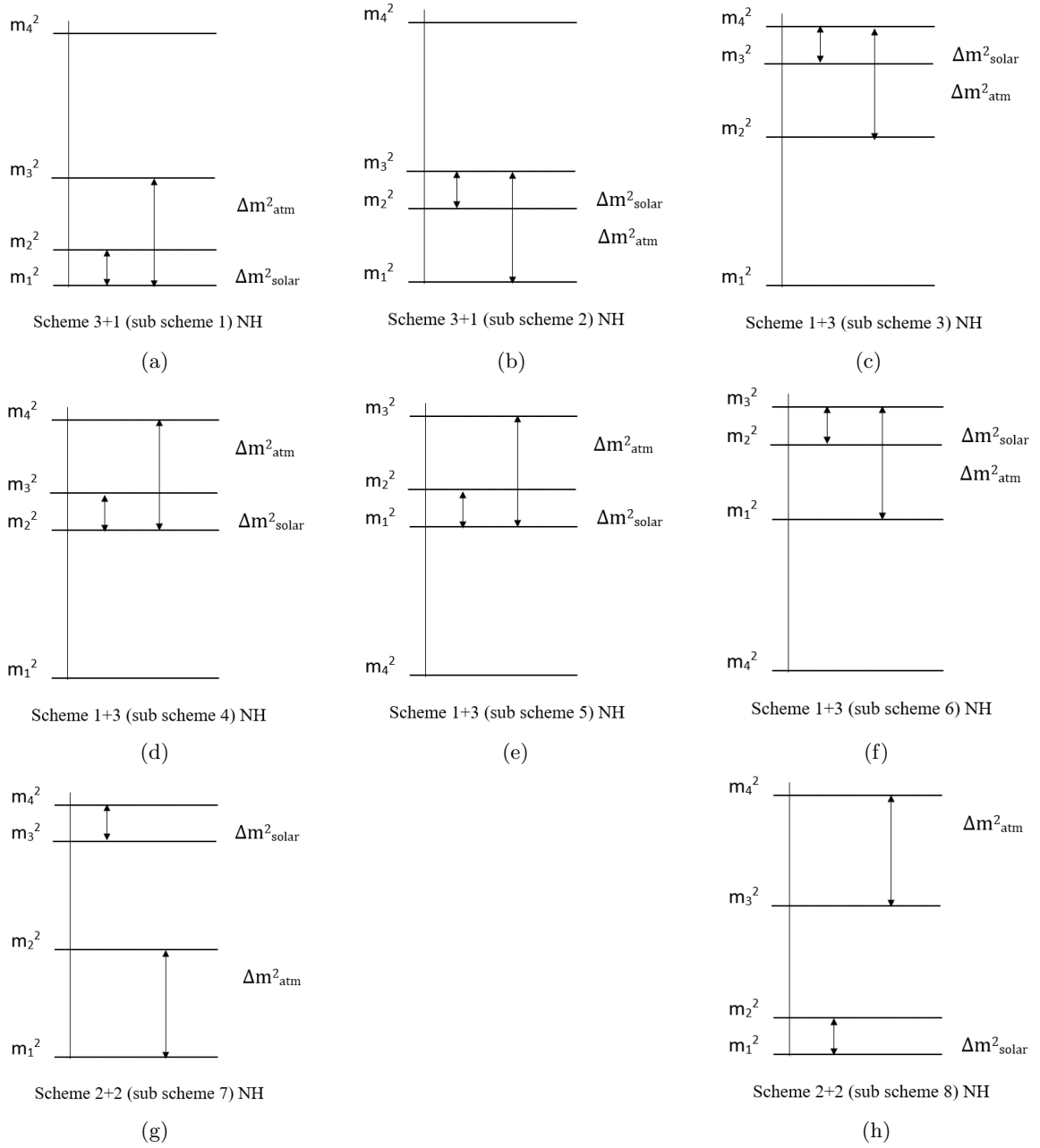


Figure 1: Different Sub schemes in 3+1, 1+3 and 2+2 Schemes (NH)

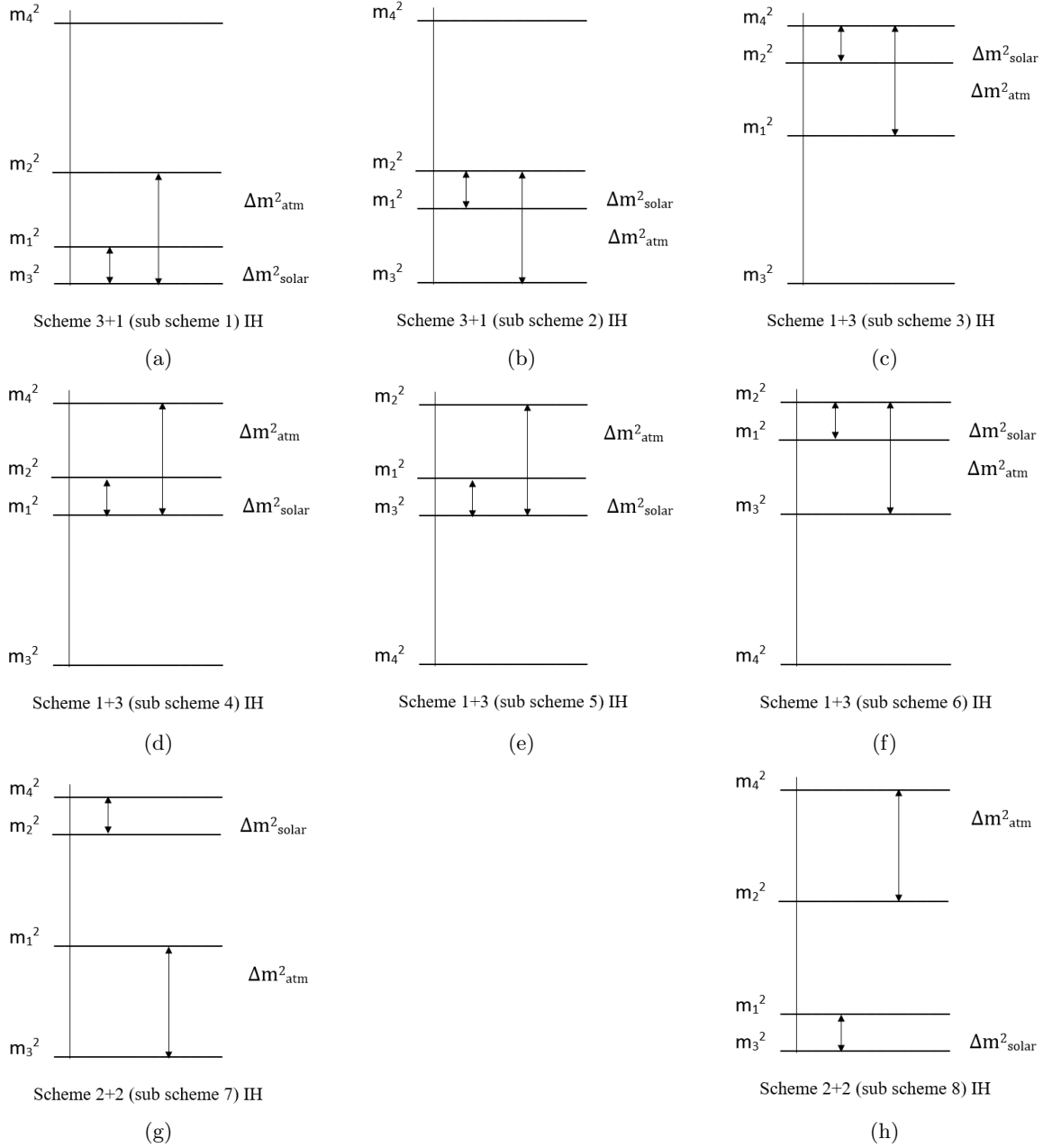


Figure 2: Different Sub schemes in 3+1, 1+3, 2+2 Schemes (IH)

In 1+3 scheme (3, 4), the sterile neutrino oscillates with one active neutrino and mass squared differences are of the order of $10^{-5}eV^2$ and $10^{-3}eV^2$, respectively. However, the LSND anomaly suggests that the third mass squared difference is approximately of the order of $1 eV^2$. If we consider the oscillations of one active and sterile neutrino with mass squared differences of order of $10^{-5}eV^2$ and $10^{-3}eV^2$, respectively then the sum of masses of three active neutrinos is disallowed by cosmological bounds [59]. Similarly, the 2+2 scheme (7, 8) is also incompatible for the same reason [51]. The sub schemes 5 and 6 of 1+3 scheme are not allowed by the LSND anomaly because the extra light mass state sterile neutrino and the active neutrino cannot have a mass squared difference of the order of $1 eV^2$.

Finally for the most viable 3+1 scheme, the mass squared differences $\Delta m_{\text{solar}}^2$ and Δm_{atm}^2 are shown below in the tabular form with NH and IH for sub scheme 1 and 2, as

Sub scheme	Mass Squared Differences
NH-1	$\Delta m_{21}^2 = \Delta m_{\text{solar}}^2, \quad \Delta m_{31}^2 = \Delta m_{\text{atm}}^2$
NH-2	$\Delta m_{32}^2 = \Delta m_{\text{solar}}^2, \quad \Delta m_{31}^2 = \Delta m_{\text{atm}}^2$
IH-1	$\Delta m_{13}^2 = \Delta m_{\text{solar}}^2, \quad \Delta m_{23}^2 = \Delta m_{\text{atm}}^2$
IH-2	$\Delta m_{21}^2 = \Delta m_{\text{solar}}^2, \quad \Delta m_{23}^2 = \Delta m_{\text{atm}}^2$

Table 1: Mass-squared differences in the 3+1 neutrino sub schemes

3 Effective Majorana Mass in 3+1 Schemes

The effective Majorana mass for three neutrinos is defined by the following equation

$$m_{\beta\beta}^{3\nu} = \sum_{j=1}^3 U_{ej}^2 m_j = \sum_{j=1}^3 |U_{ej}|^2 e^{2i\phi_j} m_j, \quad (1)$$

where U_{ej} are the elements of PMNS matrix and $\phi_j = \arg U_{ej}$. The inclusion of the sterile neutrino introduces modifications to the mixing angle and alterations in the Pontecorvo-Maki-Nakagawa-Sakata (PMNS) matrix as

$$U = R_{34} \tilde{R}_{24} \tilde{R}_{14} R_{23} \tilde{R}_{13} R_{12} P, \quad (2)$$

where the matrices R_{ij} are rotations in the ij space, e.g.

$$\tilde{R}_{14} = \begin{pmatrix} c_{14} & 0 & 0 & s_{14}e^{-i\delta_{14}} \\ 0 & 1 & 0 & 0 \\ 0 & 0 & 1 & 0 \\ -s_{14}e^{i\delta_{14}} & 0 & 0 & c_{14} \end{pmatrix},$$

$$R_{34} = \begin{pmatrix} 1 & 0 & 0 & 0 \\ 0 & 1 & 0 & 0 \\ 0 & 0 & c_{34} & s_{34} \\ 0 & 0 & -s_{34} & c_{34} \end{pmatrix}.$$

Here δ_{ij} , s_{ij} and c_{ij} are the Dirac CP- violating phases, $\sin\theta_{ij}$ and $\cos\theta_{ij}$, respectively. The matrix P is described by the three Majorana phases α , β , and γ as

$$P = \begin{pmatrix} 1 & 0 & 0 & 0 \\ 0 & e^{i\alpha/2} & 0 & 0 \\ 0 & 0 & e^{i(\beta/2+\delta_{13})} & 0 \\ 0 & 0 & 0 & e^{i(\gamma/2+\delta_{14})} \end{pmatrix}.$$

There are total three Dirac CP-violating phases δ_{ij} . The P matrix constructed in such a way that only Majorana phases will show up in the effective Majorana mass governing neutrinoless double beta decay [57]. By extending the Eq. (1), the effective Majorana mass formula for four neutrinos is

$$m_{\beta\beta}^{4\nu} = \sum_{j=1}^4 U_{ej}^2 m_j, \quad (3)$$

$$m_{\beta\beta}^{4\nu} = |U_{e1}|^2 m_1 + |U_{e2}|^2 m_2 e^{i\alpha} + |U_{e3}|^2 m_3 e^{i\beta} + |U_{e4}|^2 m_4 e^{i\gamma}. \quad (4)$$

In Eq. (4) m_1, m_2, m_3, m_4 are the masses of neutrinos. After using the values of U_{e1}, U_{e2}, U_{e3} , and U_{e4} from PMNS matrix, the Eq. (4) is modified as

$$m_{\beta\beta}^{4\nu} = [(c_{13}^2 c_{12}^2 c_{14}^2 m_1 + c_{13}^2 s_{12}^2 c_{14}^2 m_2 \cos \alpha + s_{13}^2 c_{14}^2 m_3 \cos \beta + s_{14}^2 m_4 \cos \gamma)^2 + (c_{13}^2 s_{12}^2 c_{14}^2 m_2 \sin \alpha + s_{13}^2 c_{14}^2 m_3 \sin \beta + s_{14}^2 m_4 \sin \gamma)^2]^{1/2}. \quad (5)$$

For normal hierarchy, m_1 is the lightest mass and for inverted hierarchy, m_3 is the lightest mass. The forms of effective Majorana mass for four neutrino schemes in NH and IH are as follows

3.1 3+1 Scheme (NH)

For sub scheme 1

$$m_{\beta\beta}^{4\nu} = \left[(c_{13}^2 c_{12}^2 c_{14}^2 m_1 + c_{13}^2 s_{12}^2 c_{14}^2 \sqrt{\Delta m_{solar}^2 + m_1^2} \cos \alpha + s_{13}^2 c_{14}^2 \sqrt{\Delta m_{atm}^2 + m_1^2} \cos \beta + s_{14}^2 \sqrt{\Delta m_{41}^2 + m_1^2} \cos \gamma)^2 + (c_{13}^2 s_{12}^2 c_{14}^2 \sqrt{\Delta m_{solar}^2 + m_1^2} \sin \alpha + s_{13}^2 c_{14}^2 \sqrt{\Delta m_{atm}^2 + m_1^2} \sin \beta + s_{14}^2 \sqrt{\Delta m_{41}^2 + m_1^2} \sin \gamma)^2 \right]^{1/2}. \quad (6)$$

For sub scheme 2

$$m_{\beta\beta}^{4\nu} = \left[(c_{13}^2 c_{12}^2 c_{14}^2 m_1 + c_{13}^2 s_{12}^2 c_{14}^2 \sqrt{\Delta m_{atm}^2 - \Delta m_{solar}^2 + m_1^2} \cos \alpha + s_{13}^2 c_{14}^2 \sqrt{\Delta m_{atm}^2 + m_1^2} \cos \beta + s_{14}^2 \sqrt{\Delta m_{41}^2 + m_1^2} \cos \gamma)^2 + (c_{13}^2 s_{12}^2 c_{14}^2 \sqrt{\Delta m_{atm}^2 - \Delta m_{solar}^2 + m_1^2} \sin \alpha + s_{13}^2 c_{14}^2 \sqrt{\Delta m_{atm}^2 + m_1^2} \sin \beta + s_{14}^2 \sqrt{\Delta m_{41}^2 + m_1^2} \sin \gamma)^2 \right]^{1/2}. \quad (7)$$

The forms of effective Majorana mass for different schemes in IH are as follows

3.2 3+1 Scheme (IH)

For sub scheme 1

$$\begin{aligned}
m_{\beta\beta}^{4\nu} = & \left[(c_{13}^2 c_{12}^2 c_{14}^2 \sqrt{\Delta m_{solar}^2 + m_3^2} + c_{13}^2 s_{12}^2 c_{14}^2 \sqrt{\Delta m_{atm}^2 + m_3^2} \cos \alpha + s_{13}^2 c_{14}^2 m_3 \cos \beta \right. \\
& + s_{14}^2 \sqrt{\Delta m_{43}^2 + m_3^2} \cos \gamma)^2 + (c_{13}^2 s_{12}^2 c_{14}^2 \sqrt{\Delta m_{atm}^2 + m_3^2} \sin \alpha \\
& \left. + s_{13}^2 c_{14}^2 m_3 \sin \beta + s_{14}^2 \sqrt{\Delta m_{43}^2 + m_3^2} \sin \gamma)^2 \right]^{1/2}.
\end{aligned} \tag{8}$$

For sub scheme 2

$$\begin{aligned}
m_{\beta\beta}^{4\nu} = & \left[(c_{13}^2 c_{12}^2 c_{14}^2 \sqrt{m_{atm}^2 - \Delta m_{solar}^2 + m_3^2} + c_{13}^2 s_{12}^2 c_{14}^2 \sqrt{\Delta m_{atm}^2 + m_3^2} \cos \alpha + s_{13}^2 c_{14}^2 m_3 \cos \beta \right. \\
& + s_{14}^2 \sqrt{\Delta m_{43}^2 + m_3^2} \cos \gamma)^2 + (c_{13}^2 s_{12}^2 c_{14}^2 \sqrt{\Delta m_{atm}^2 + m_3^2} \sin \alpha \\
& \left. + s_{13}^2 c_{14}^2 m_3 \sin \beta + s_{14}^2 \sqrt{\Delta m_{43}^2 + m_3^2} \sin \gamma)^2 \right]^{1/2}.
\end{aligned} \tag{9}$$

4 Results and Discussions

The $m_{\beta\beta}$ as calculated by using Eq. (5) clearly depends on mass eigenvalues, neutrino mixing angles and Majorana phases α , β and γ . We used the values of these parameters as given in Table 2. In the computation, the lightest neutrino mass m_{lightest} i.e., m_1 for normal hierarchy and m_3 for inverted hierarchy are allowed to vary randomly in the range $(10^{-5} - 1) eV$. The mass of sterile neutrino (m_4) is calculated corresponding to the m_{lightest} . The unknown Majorana phases (α, β and γ) are freely allowed to vary randomly from 0° - 360° . The third mass squared difference is explored randomly in the range $(1.1 - 2.4) eV^2$ and at the best fit value, i.e., 1.73 [45]. The third mass-squared difference, $\Delta m_{14}^2 = (7.3 \pm 1.17) eV^2$, reported by the NEUTRINO-4 experiment, is also considered in this study.

We have used the 1σ level, 3σ level and best fit values for the parameters Δm_{solar}^2 , Δm_{atm}^2 , θ_{12} , θ_{13} and θ_{14} as per given in the Table 2.

Parameter	best-fit $\pm 1\sigma$ range (NH)	best-fit $\pm 1\sigma$ range (IH)	3σ range (NH)	3σ range (IH)
$\sin^2 \theta_{12}$	$0.307_{-0.011}^{+0.012}$	$0.308_{-0.011}^{+0.012}$	0.275 - 0.345	0.275 - 0.345
$\sin^2 \theta_{23}$	$0.561_{-0.015}^{+0.012}$	$0.562_{-0.015}^{+0.012}$	0.430 - 0.596	0.437 - 0.597
$\sin^2 \theta_{13}$	$0.02195_{-0.00058}^{+0.00054}$	$0.02224_{-0.00057}^{+0.00056}$	0.02023 - 0.02376	0.02053 - 0.02397
$\Delta m_{atm}^2 / 10^{-3} eV^2$	$2.534_{-0.023}^{+0.025}$	$-2.510_{-0.025}^{+0.024}$	2.463 - 2.606	-2.584 - -2.438
$\Delta m_{solar}^2 / 10^{-5} eV^2$	$7.49_{-0.19}^{+0.19}$	$7.49_{-0.19}^{+0.19}$	6.92 - 8.05	6.92 - 8.05
$\Delta m_{4s}^2 / eV^2$	1.73	1.73	1.1 - 2.4	1.1 - 2.4

Table 2: The neutrino oscillation data from global fits used in the numerical analysis. The parameter s in $\Delta m_{4s}^2 / eV^2$ takes the value $s = 1$ for NH and $s = 3$ for IH [45, 60]

The variation of $m_{\beta\beta}$ as a function of m_{lightest} and sum of neutrino masses Σ in the 3+1 scheme for normal hierarchy is shown in Fig. (3). The horizontal lines denote the experimental ranges of different experiments like KamLAND-Zen and GERDA [5, 6, 8], CUORE [9, 10], LEGEND [11] and nEXO [12].

The vertical lines in the figures (left panels) denote the current and future ranges for m_{lightest} , given by the KATRIN experiment i.e. 0.8 eV (current limit) and 0.2 eV (future limit) [61]. These lines are included in plots illustrating the $m_{\beta\beta}$ as a function of m_{lightest} . However, the vertical line in the figures (right panels) depicts the cosmological bounds on the sum of three neutrino masses [59].

These lines are included in plots illustrating the $m_{\beta\beta}$ as a function of sum of neutrino masses i.e. Σ . The analysis of Fig. (3) (a) shows the effective Majorana mass, i.e., $m_{\beta\beta}$ for sub scheme 1 (NH) is consistent with present and future experimental data ranges. It can be observed from Fig. (3) (b) that the sum of four neutrino masses at 3σ level is limited to the interval between (1.11 – 4.81) eV (depicted by red region) and the sum of four neutrino masses at 1σ level is limited to the interval between (1.41 – 4.71) eV (depicted by blue region). The sum of three neutrino masses at 3σ level in sub scheme 1 is confined to the interval between (0.06 – 3.33) eV (illustrated by green region) and the sum of three neutrino masses at 1σ level is confined to the interval between (0.06 – 3.21) eV (illustrated by yellow region).

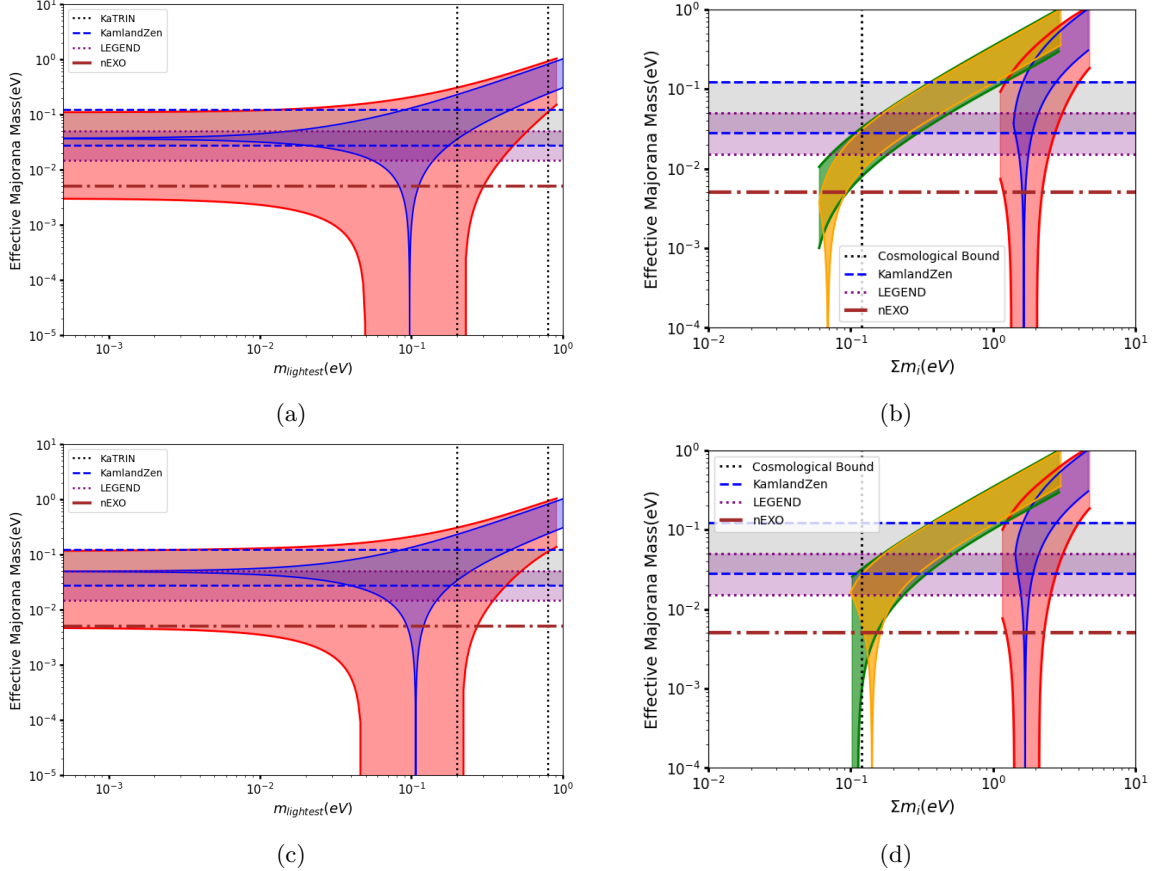


Figure 3: Effective Majorana mass as a function of lightest mass m_{lightest} (a, c) and sum of masses Σ (b, d) for 3+1 scheme (NH) for 1σ and 3σ ranges

The bound on mass of sterile neutrino is calculate from Fig. (3) (b) which is (0.99 – 4.75) eV at 3σ level and (1.29 – 4.65) eV at 1σ level. However, the numerically calculated range for mass of sterile neutrino is more constrained i.e. (1.04 – 1.55) eV at 3σ level and (1.31 – 1.32) eV at 1σ level.

Fig. (3) (c) analysis shows the $m_{\beta\beta}$ for sub scheme 2 (NH) is consistent with present and future experimental data ranges. It can be observed from Fig. (3) (d) that the sum of four neutrino masses at 3σ level is limited to the interval between (1.15 – 4.81) eV (depicted by red region) and the sum of four neutrino masses at 1σ level is limited to the interval between (1.42 – 4.69) eV (depicted by blue region). The sum of three neutrino masses at 3σ level in sub scheme 2 (NH) is limited to the interval between (0.10 – 2.94) eV (illustrated by green region) and the sum of three neutrino masses

at 1σ level is limited to the range between $(0.10 - 2.94)$ eV (illustrated by yellow region). The bound on mass of sterile neutrino is calculate from Fig. (3) (d) which is $(1.03 - 4.71)$ eV at 3σ level and $(1.30 - 4.60)$ eV at 1σ level. However, the numerically calculated range for mass of sterile neutrino is more constrained i.e. $(1.04 - 1.55)$ eV at 3σ level and $(1.31 - 1.32)$ eV at 1σ level. Consequently, this theoretical framework demonstrates feasibility in light of both current and future experimental outcomes.

The analysis of Fig. (4) (a) shows the $m_{\beta\beta}$ for sub scheme 1 (IH) is consistent with present and future experimental data ranges. Similar behavior has been observed in the plots presented in Ref. [42].

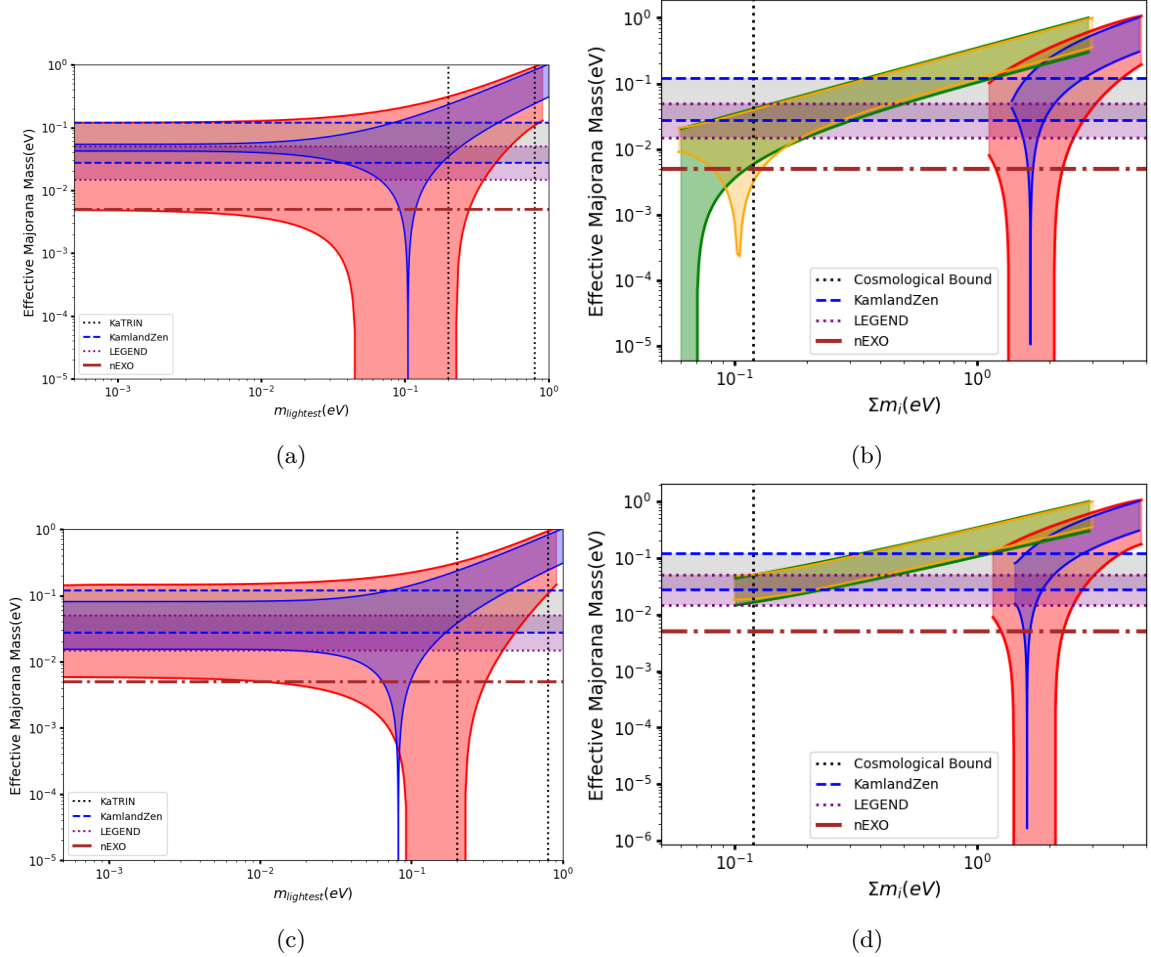


Figure 4: Effective Majorana mass as a function of lightest mass m_{lightest} (a, c) and sum of masses Σ (b, d) for 3+1 scheme (IH) for 1σ and 3σ ranges

It can be observed from Fig. (4) (b) that the sum of four neutrino masses at 3σ level is limited to the interval between $(1.14 - 4.78)$ eV (depicted by red region) and the sum of four neutrino masses at 1σ level is limited to the interval between $(1.35 - 4.62)$ eV (depicted by blue region). The sum of three neutrino masses at 3σ level in sub scheme 1 (IH) is confined to the range between $(0.06 - 2.99)$ eV (illustrated by green region) and the sum of three neutrino masses at 1σ level is limited to the range between $(0.06 - 2.89)$ eV (illustrated by yellow region). The bound on mass of sterile neutrino is calculate from Fig. (4) (b) which is $(1.02 - 4.72)$ eV at 3σ level and $(1.23 - 4.56)$ eV at 1σ level. However, the numerically calculated range for mass of sterile neutrino is more constrained i.e.

(1.05 – 1.55) eV at 3σ level and (1.31 – 1.32) eV at 1σ level.

Fig. (4) (c) analysis shows the $m_{\beta\beta}$ for sub scheme 2 (IH) for inverted hierarchy is consistent with present and future experimental data ranges. It can be observed from Fig. (4) (d) that the sum of four neutrino masses at 3σ level is limited to the interval between (1.16 – 4.75) eV (depicted by red region) and the sum of four neutrino masses at 1σ level is limited to the interval between (1.43 – 4.61) eV (depicted by blue region). The sum of three neutrino masses at 3σ level in sub scheme 2 (IH) is confined to the interval between (0.09 – 2.99) eV (illustrated by green region) and the sum of three neutrino masses at 1σ level is confined to the interval between (0.09 – 2.89) eV (illustrated by yellow region). The bound on mass of sterile neutrino is calculate from Fig. (4) (d) which is (1.04 – 4.66) eV at 3σ level and (1.31 – 4.32) eV at 1σ level. However, the numerically calculated range for mass of sterile neutrino is more constrained i.e. (1.05 – 1.55) eV at 3σ level and (1.31 – 1.32) eV at 1σ level. Consequently, this theoretical framework demonstrates feasibility in light of both current and future experimental results.

We summarize the limits on $\Sigma(4\nu)$, i.e. sum of four neutrino masses numerically calculated limits on m_4 , limits on three neutrino mass and graphically calculated limit on m_4 in Table 3 and Table 4 as

Scheme	Ordering	Limits on $\Sigma(4\nu)$ (eV)				Numerically calculated limits on m_4 (eV)			
		1σ		3σ		1σ		3σ	
	sub schemes	1	2	1	2	1	2	1	2
3+1	NH	1.41-4.71	1.42-4.69	1.11-4.81	1.15-4.81	1.31-1.32	1.31-1.32	1.04-1.55	1.04-1.55
	IH	1.35-4.62	1.43-4.61	1.14-4.78	1.16-4.75	1.31-1.32	1.31-1.32	1.05-1.55	1.05-1.55

Table 3: Limits on $\Sigma(4\nu)$ and numerically calculated limits on m_4 by using third mass squared difference and m_{lightest} in 3+1 scheme for 1σ and 3σ ranges

Scheme	Ordering	Limits on sum of three neutrino masses (eV)				Graphically calculated limit on m_4 (eV)			
		1σ		3σ		1σ		3σ	
	sub schemes	1	2	1	2	1	2	1	2
3+1	NH	0.06-3.21	0.10-2.94	0.06-3.33	0.10-2.94	1.29-4.65	1.30-4.60	0.99-4.75	1.03-4.71
	IH	0.06-2.89	0.09- 2.89	0.06-2.99	0.09-2.99	1.23-4.56	1.31-4.32	1.02-4.72	1.04-4.66

Table 4: Limits on sum of three neutrino masses and graphically calculated limits on m_4 (difference between the sum of four neutrino masses and three neutrino masses) in 3+1 scheme for 1σ and 3σ ranges

The analysis of $m_{\beta\beta}$ with respect to the lightest neutrino mass is also performed using predictions from the NEUTRINO-4 experiment. The fig. 5(a) indicates that sub scheme 1 (NH) is consistent with the KamLAND-Zen experimental results. Additionally, the corresponding lightest neutrino mass shows compatibility with the current KATRIN limits, but is not consistent with the proposed sensitivity of the KATRIN experiment. In future, the proposed sensitivity of KATRIN experiment will rule out this scenario. The sub scheme 2 (NH) in Fig. 5(b) also exhibits similar results as sub scheme 1.

In Fig. 6, both sub schemes 1 and 2 demonstrate that $m_{\beta\beta}$, as a function of the lightest neutrino mass, is compatible with the KamLAND-Zen limits. Moreover, the lightest neutrino mass is compatible with the current KATRIN limits but shows incompatibility with the proposed sensitivity of KATRIN experiment. The NEUTRINO-4 experiment shows insensitivity towards the neutrino mass hierarchy because in both the normal hierarchy and inverted hierarchy the dominant term arises from the third mass squared difference, which is of the same magnitude in both cases. Therefore, the NEUTRINO-4

experiment cannot distinguish between normal and inverted hierarchies of neutrinos.

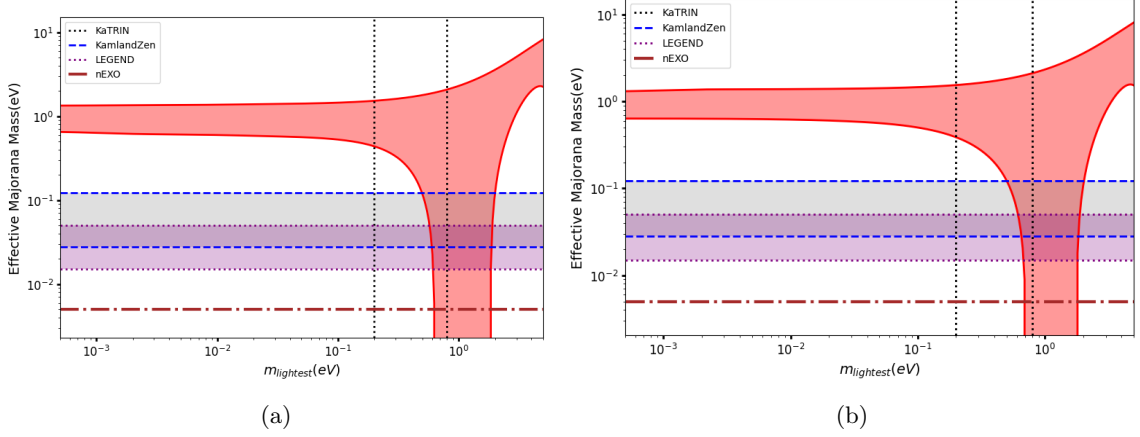


Figure 5: Effective Majorana mass as a function of lightest mass m_{lightest} for 3+1 scheme (NH) for 3σ ranges with third mass squared difference predicted by the NEUTRINO-4 experiment

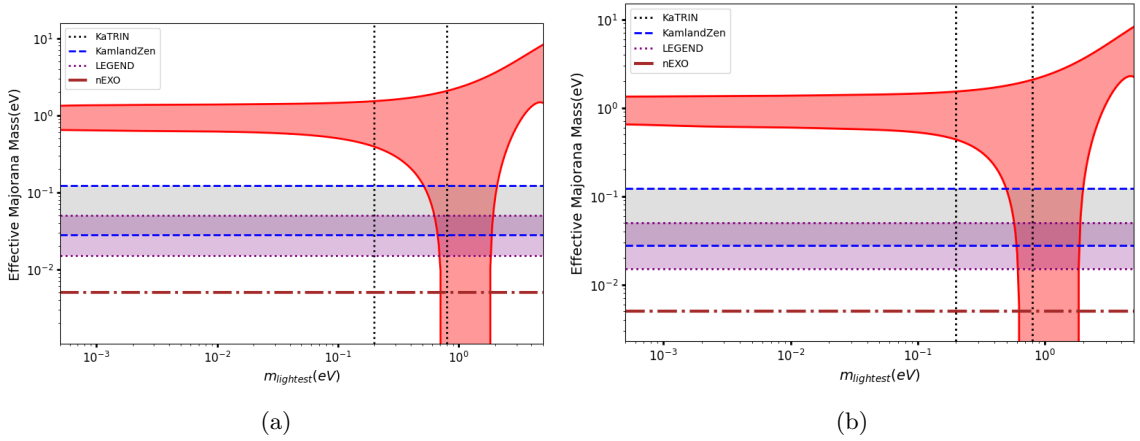


Figure 6: Effective Majorana mass as a function of lightest mass m_{lightest} for 3+1 scheme (IH) for 3σ ranges with third mass squared difference predicted by the NEUTRINO-4 experiment

5 Conclusions

In this work, we assumed a sterile neutrino mixed with three active neutrinos and investigated the third mass squared difference in the 3σ range, i.e., $1.1 - 2.4 \text{ eV}^2$ and at best fit value, i.e., 1.73 eV^2 . We used the global fits of the current understanding of neutrino mass squared differences and mixing angles, recent and future experiments on the effective Majorana mass, neutrino absolute mass scale experiments and reactor experiments data in our study. In the possible different active-sterile schemes such as 3+1, 1+3 and 2+2, we confirmed that recent and future experimental data support 3+1 scheme only in both the normal as well as inverted hierarchies of neutrino masses. As also observed, as in the existing literature, the other two schemes 1+3 and 2+2 are not found favoured by the experimental data. Using the 3+1 scheme, the upper limit on the mass of sterile neutrino is obtained as 4.75 eV for normal hierarchy and 4.72 eV for inverted hierarchy at 3σ level. However, upper limits on the sum of four neutrino masses are 4.81 eV for NH and 4.78 eV for IH at 3σ

level. Since for both the hierarchies the limits of sum of four neutrino masses, thus obtained, are almost similar, therefore, the four neutrino study will not help us in distinguishing between the mass hierarchy of neutrinos.

In the work, we also investigated the effective Majorana mass in light of the NEUTRINO-4 experiment, which shows that the current experimental bounds provided by KamLAND-Zen are compatible with the effective Majorana mass limits. In this case, the lightest neutrino mass is also compatible with the current limit of the KATRIN experiment. However, at this stage, the proposed sensitivity of the KATRIN experiment rules out this scenario, and this will show significant tension with the stringent bound set by the KamLAND-Zen experiment. As we know, the effective Majorana mass depends on mass eigenvalues, neutrino mixing angles and Majorana phases α , β and γ , these parameters are shaping the overall understanding of effective Majorana mass within the proposed schemes. The detailed results and limits on mass of sterile neutrinos are shown in the Table 3 and Table 4.

The sterile neutrinos of eV scale are one of the most intriguing possibilities in the search for right handed helicity of neutrinos beyond the Standard Model. Anomalous results from short-baseline experiments have exciting indications, which cannot be explained in the standard framework of 3ν mixing. Furthermore, the 3+1 scheme has been considered as the most promising framework to be tested in the short-baseline neutrino oscillations.

After the emergence the reactor antineutrino anomaly (RAA) [62], several projects have been proposed to search out the sterile neutrinos of eV mass scale. To resolve the LSND, MiniBooNE and Gallium anomalies, an intense experimental activities have been carried out worldwide. The experiments e.g. NEOS/ Daya Bay [63], DANSS [64], STEREO [65], PROSPECT [66] and SoLiD [67] are already in operation and taking data [68]. The PROSPECT-I aims to measure the signatures of sterile neutrino oscillations, excludes the 3+1 sterile neutrino parameter space above 3 eV^2 that was previously unexplored by other neutrino experiments at 95% C.L [69].

The preliminary results are excluding part of the allowed range of parameters, but also giving positive hints for the new oscillation signals. Apart from this, there are several experiments keeping eyes on the signals of $0\nu\beta\beta$ decay, which have been depicted on the plots shown in the work.

We are keen to see the exciting results from the new short-baseline neutrino experimental programs and experiments targeting to $0\nu\beta\beta$ decay in the near future that would enlighten us more on the existence of eV-scale sterile neutrinos and settle the longstanding issue of $0\nu\beta\beta$ decay.

Acknowledgements

The authors are thankful to the Inter University Centre for Astronomy and Astrophysics (IUCAA), Pune for providing necessary facilities during the completion of this work.

References

- [1] D. Q. Adams *et al.* [CUORE], Phys. Rev. Lett. **124**, no.52, 122501 (2020).
- [2] J. Singh, Adv. High Energy Phys. **2019**, 4863620 (2019).

- [3] W. H. Furry, Phys. Rev. **56**, 1184-1193 (1939).
- [4] M. J. Dolinski, A. W. P. Poon and W. Rodejohann, Ann. Rev. Nucl. Part. Sci. **69**, 219-251 (2019).
- [5] J. Shirai [Kamland-Zen], PoS **HQL2018**, 050 (2018).
- [6] J. Shirai [KamLAND-Zen], J. Phys. Conf. Ser. **888**, no.5, 012031 (2017).
- [7] S. Abe *et al.* [KamLAND-Zen], [arXiv:2406.11438 [hep-ex]].
- [8] I. Nutini, D. Q. Adams, C. Alduino *et al.* Int. J. Mod. Phys. A **37**, no.07, 2240014 (2022).
- [9] M. Agostini *et al.* [GERDA], Phys. Rev. Lett. **120**, no.13, 132503 (2018).
- [10] A. Campani *et al.* [CUORE], Int. J. Mod. Phys. A **35**, no.36, 2044016 (2020).
- [11] N. Abgrall *et al.* [LEGEND], AIP Conf. Proc. **1894**, no.1, 020027 (2017).
- [12] G. Adhikari *et al.* [nEXO], J. Phys. G **49**, no.1, 015104 (2022).
- [13] B. J. P. Jones, [arXiv:2108.09364 [nucl-ex]].
- [14] A. Gando *et al.* [KamLAND-Zen], Phys. Rev. Lett. **117**, no.8, 082503 (2016).
- [15] F. Capozzi, E. Lisi, A. Marrone and A. Palazzo, Prog. Part. Nucl. Phys. **102**, 48-72 (2018).
- [16] B. Dasgupta and J. Kopp, Phys. Rept. **928**, 1-63 (2021).
- [17] G. B. Mills [LSND], Nucl. Phys. B Proc. Suppl. **66**, 382-386 (1998).
- [18] W. C. Louis, Prog. Part. Nucl. Phys. **63**, 51-73 (2009).
- [19] M. A. Acero, C. Giunti and M. Laveder, Phys. Rev. D **78**, 073009 (2008).
- [20] C. Giunti and M. Laveder, Phys. Rev. C **83**, 065504 (2011).
- [21] K. Abe *et al.* [T2K], Nucl. Instrum. Meth. A **659**, 106-135 (2011).
- [22] C. C. Polly, Nucl. Phys. B Proc. Suppl. **217**, 183-185 (2011).
- [23] A. A. Aguilar-Arevalo *et al.* [MiniBooNE], Phys. Rev. Lett. **110**, 161801 (2013).
- [24] A. A. Aguilar-Arevalo *et al.* [MiniBooNE], Phys. Rev. D **103**, no.5, 052002 (2021).
- [25] S. N. Gninenko, Phys. Rev. D **83**, 015015 (2011).
- [26] G. Drexlin, Nucl. Phys. B Proc. Suppl. **118**, 146-153 (2003).
- [27] K. Eitel [KARMEN], Nucl. Phys. B Proc. Suppl. **91**, 191-197 (2001).
- [28] R. Acciarri *et al.* [MicroBooNE], JINST **12**, no.02, P02017 (2017).
- [29] A. M. Abdullahi *et al.* [MicroBooNE], [arXiv:2502.10900 [hep-ex]].
- [30] P. Abratenko *et al.* [MicroBooNE], Phys. Rev. Lett. **130**, no.1, 011801 (2023).
- [31] P. B. Denton, Phys. Rev. Lett. **129**, no.6, 061801 (2022).
- [32] V. V. Barinov, S. N. Danshin, *et al.* Phys. Rev. C **105**, no.6, 065502 (2022).

- [33] A. P. Serebrov, R. M. Samoilov, *et al.* JETP Lett. **116**, no.10, 669-682 (2022).
- [34] A. P. Serebrov, R. M. Samoilov, *et al.* Phys. Rev. D **104**, no.3, 032003 (2021).
- [35] V. A. Naumov and D. S. Shkirmanov, Universe **7**, no.7, 246 (2021).
- [36] M. Danilov *et al.* [DANSS], PoS **EPS-HEP2021**, 241 (2022).
- [37] Y. J. Ko *et al.* [NEOS], Phys. Rev. Lett. **118**, no.12, 121802 (2017).
- [38] T. Abrahão *et al.* [Double Chooz], Eur. Phys. J. C **81**, no.8, 775 (2021).
- [39] J. H. Choi *et al.* [RENO], Phys. Rev. Lett. **125**, no.19, 191801 (2020).
- [40] F. P. An *et al.* [Daya Bay], Phys. Rev. Lett. **133**, no.5, 051801 (2024).
- [41] I. Esteban, M. C. Gonzalez-Garcia, *et al.* JHEP **12**, 216 (2024).
- [42] C. Giunti and E. M. Zavanin, JHEP **07**, 171 (2015).
- [43] S. Goswami, D. Pachhar and S. Pan, Phys. Rev. D **110**, no.1, 015028 (2024).
- [44] S. Goswami and W. Rodejohann, Phys. Rev. D **73**, 113003 (2006).
- [45] S. Gariazzo, C. Giunti, M. Laveder and Y. F. Li, JHEP **06**, 135 (2017).
- [46] Y. F. Li and S. s. Liu, Phys. Lett. B **706**, 406-411 (2012).
- [47] N. Nath, M. Ghosh and S. Gupta, Int. J. Mod. Phys. A **31**, no.24, 1650132 (2016).
- [48] S. Verma, Mod. Phys. Lett. A **31**, no.06, 1650040 (2016).
- [49] N. Gaur, A. Ghosal, E. Ma and P. Roy, Phys. Rev. D **58**, 071301 (1998).
- [50] O. Yasuda, PTEP **2022**, no.12, 12B105 (2022).
- [51] M. Maltoni, T. Schwetz, M. A. Tórtola *et al.* Nucl. Phys. B Proc. Suppl. **143**, 523-523 (2005).
- [52] J. Singh, Adv. High Energy Phys. **2019**, 4863620 (2019).
- [53] S. Mohanty, D. P. Roy and U. Sarkar, Phys. Lett. B **445**, 185-190 (1998).
- [54] B. Singh Koranga and V. K. Nautiyal, Int. J. Theor. Phys. **60**, no.3, 781-792 (2021).
- [55] E. Ma and P. Roy, Phys. Rev. D **52**, R4780-R4783 (1995).
- [56] W. Dekens, J. de Vries, D. Castillo, J. Menéndez, *et al.* [arXiv:2402.07993 [hep-ph]].
- [57] J. Barry, W. Rodejohann and H. Zhang, JHEP **07**, 091 (2011).
- [58] S. M. Bilenky, S. Pascoli and S. T. Petcov, Phys. Rev. D **64**, 113003 (2001).
- [59] N. Aghanim *et al.* [Planck], Astron. Astrophys. **641**, A6 (2020).
- [60] I. Esteban, M. C. Gonzalez-Garcia, *et al.* JHEP **12**, 216 (2024).
- [61] M. Aker *et al.* [KATRIN], J. Phys. G **49**, no.50, 100501 (2022).
- [62] G. Mention, M. Fechner, T. Lasserre, T. A. Mueller, *et al.* Phys. Rev. D **83**, 073006 (2011).

- [63] Y. J. Ko *et al.* [NEOS], Phys. Rev. Lett. **118**, no.12, 121802 (2017).
- [64] I. Alekseev, V. Belov, V. Brudanin, M. Danilov, *et al.* JINST **11**, no.11, P11011 (2016).
- [65] N. Allemandou *et al.* [STEREO], JINST **13**, no.07, P07009 (2018).
- [66] J. Ashenfelter *et al.* [PROSPECT], J. Phys. G **43**, no.11, 113001 (2016).
- [67] V. Pestel [SoLid], PoS **EPS-HEP2017**, 511 (2018).
- [68] A. Minotti, PoS **TAUP2023**, 208 (2024).
- [69] M. Andriamirado *et al.* [PROSPECT], [arXiv:2406.10408 [hep-ex]].